Article details

Wielstra B., Zielinski P. & Babik W. (2017), The Carpathians hosted extra-Mediterranean refugia-within-refugia during the Pleistocene Ice Age: genomic evidence from two newt genera, Biological Journal of the Linnean Society 122(3): 605-613.
Doi: 10.1093/biolinnean/blx087

Biological Journal of the Linnean Society, 2017, **122**, 605–613. With 1 figure.

The Carpathians hosted extra-Mediterranean refugia-within-refugia during the Pleistocene Ice Age: genomic evidence from two newt genera

BEN WIELSTRA[1,2,3]*, PIOTR ZIELIŃSKI[4] and WIESŁAW BABIK[4]

[1]*Department of Animal and Plant Sciences, University of Sheffield, Sheffield S10 2TN, UK*
[2]*Department of Ecology and Evolutionary Biology, University of California, Los Angeles, CA 90095, USA*
[3]*Naturalis Biodiversity Center, P.O. Box 9517, 2300 RA Leiden, The Netherlands*
[4]*Institute of Environmental Sciences, Jagiellonian University, ul. Gronostajowa 7, 30-387 Kraków, Poland*

Received 1 June 2017; revised 27 June 2017; accepted for publication 27 June 2017

Part of Europe's temperate species survived the Pleistocene glacial cycles in refugia north of the Mediterranean peninsulas. For one such extra-Mediterranean refugia, the Carpathians, an intricate 'refugia-within-refugia' scenario has been suggested, involving species surviving in multiple discrete glacial refugia. We test the Carpathian refugia-within-refugia hypothesis, employing genome-wide multilocus data sets for two newt species (*Triturus cristatus* and *Lissotriton montandoni*). We first use Bayesian clustering to delineate intraspecific evolutionary lineages. The number of intraspecific lineages identified, and the allocation of localities to these lineages, were used to construct testable hypotheses on the spatial arrangement of glacial refugia in both newt species. Next we employ approximate Bayesian computation to date whether these lineages are of Holocene (< 12 Ka) or Pleistocene (> 12 Ka) origin. We identify three intraspecific evolutionary lineages for *T. cristatus* and two for *L. montandoni*. For both newt species, intraspecific divergence is rooted in the Pleistocene, in line with species survival in distinct range fragments during the last glacial period. Hence, our findings firmly support the Carpathian refugia-within-refugia hypothesis. Furthermore, we show that mitochondrial DNA overestimates the age of intraspecific evolutionary lineages and we urge caution in basing refugia-within-refugia scenarios on mitochondrial DNA alone.

ADDITIONAL KEYWORDS: approximate Bayesian computation – Bayesian clustering – historical biogeography – *Lissotriton montandoni* – next-generation sequencing – Quaternary – *Triturus cristatus*.

INTRODUCTION

The climate oscillations of the Pleistocene Ice Age moulded intraspecific genetic structuring by repeatedly reducing temperate species' ranges during glacial cycles (Hewitt, 2000). The refugia-within-refugia concept addresses the evolution of intraspecific geographical genetic structuring, as species survive glacial conditions in fragmented pockets of suitable habitat within a single, wider refugial area (Gómez & Lunt, 2007; Abellán & Svenning, 2014). Refugia-within-refugia have been reported from Europe's canonical glacial refugia: the Iberian (Gómez & Lunt, 2007), Italian (Canestrelli *et al.*, 2014) and Balkan (Poulakakis *et al.*, 2015) Peninsulas. As regions situated north of Europe's southern peninsula are increasingly appreciated as sources of postglacial recolonization of temperate Europe (Stewart *et al.*, 2010; Schmitt & Varga, 2012), this raises the question whether such areas also facilitated intraspecific Pleistocene differentiation. The Carpathians are arguably the most significant extra-Mediterranean refugium and accumulating phylogeographic studies suggest a refugia-within-refugia scenario applies (Mráz & Ronikier, 2016). We test this hypothesis here, using two newt species from different genera as a system.

The Northern crested newt *Triturus cristatus* (Laurenti, 1768) is a species of lowland and hills, distributed over much of temperate Europe and

*Corresponding author. E-mail: ben.wielstra@naturalis.nl

adjacent Asia, while the Carpathian newt *Lissotriton montandoni* (Boulenger, 1880) is a montane species, endemic to the Carpathians (Fig. 1a). Despite their ecological differences (Speybroeck *et al.*, 2016), both species survived the Pleistocene glaciations in the Carpathians (Wielstra *et al.*, 2013; Zieliński *et al.*, 2013, 2014a; Wielstra, Babik & Arntzen, 2015). As genetic data show geographical substructuring and species distribution models suggest glacial range fragmentation within the Carpathians, these species are particularly suitable to test the Carpathian refugia-within-refugia hypothesis. We sequence several dozen nuclear DNA markers and use Bayesian clustering to delineate intraspecific geographical structure within each species. Subsequently, we test in an approximate Bayesian computation (ABC) framework whether the observed intraspecific structure indeed arose during the Pleistocene, which would indicate species survival in multiple discrete glacial refugia and thus support the Carpathian refugia-within-refugia hypothesis.

MATERIAL AND METHODS

Sampling

For *T. cristatus*, we included 28 Carpathian breeding ponds (Fig. 1b) and an additional seven positioned in postglacially colonized area and sampled up to three (2.9 on average) individuals per pond (see Table S1 in Supporting Information). For *L. montandoni*, we included 31 Carpathian breeding ponds (Fig. 1c) and sampled up to three (1.3 on average) individuals per pond (Table S2 in Supporting Information). Individual ponds were treated as localities.

Summary of sequencing

For *T. cristatus*, we newly sequenced 52 nuclear markers. See Wielstra *et al.* (2014) for a detailed description of the laboratory and bioinformatics protocol. In brief, we amplified markers of *c.* 140 bp in length (excluding primers), positioned in 3′ untranslated regions of protein-coding genes, in five multiplex PCRs. We pooled

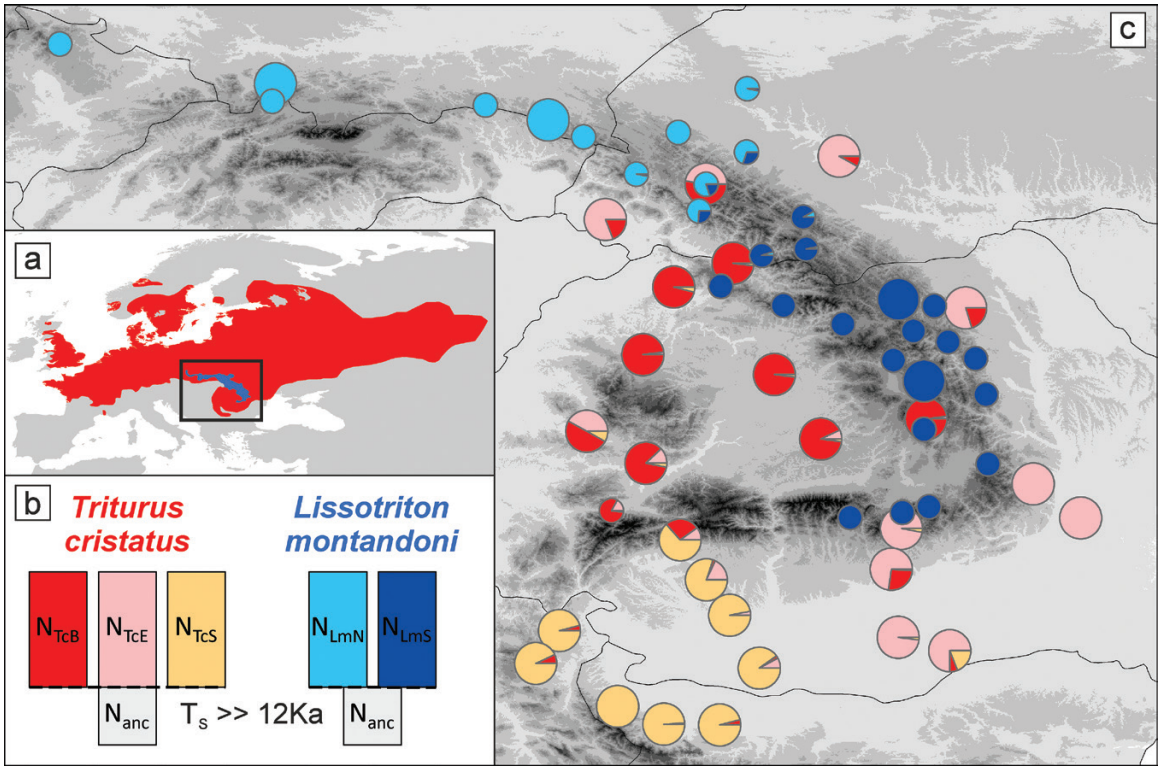

Figure 1. Distribution of and Bayesian clustering results for *Triturus cristatus* and *Lissotriton montandoni*. In (a) rough outlines of the ranges of both species are shown, with the range of *L. montandoni* (in blue) superimposed on that of *T. cristatus* (in red). In (b) the preferred model for each species in the approximate Bayesian computation analysis is shown. Codes for evolutionary lineages are explained in Results and colours correspond to the gene pools identified in the STRUCTURE analysis. In (c) pie diagrams represent the allocation by STRUCTURE of localities to different gene pools (k) for *T. cristatus* (k = 3; red tones) and *L. montandoni* (k = 2; blue tones) and pie diameter reflects sample size of localities (n = 1 or n = 3). Grey shading denotes elevation.

the multiplexes for each individual and ligated unique tags to be able to recognize the amplicons belonging to each individual. We sequenced the amplicons on the Ion Torrent next-generation sequencing platform and processed the output with a bioinformatics pipeline that filters out poor quality reads, identifies alleles and converts data to a genotypic format directly usable for population genetic analysis. Mean coverage was 777 reads (range 0–13 622) per marker-individual combination. Marker-individual combinations with ≥ 20 reads (1.73%) were considered successful.

For *L. montandoni*, we sequenced 74 nuclear markers. See Zieliński *et al.* (2014b) for a detailed description of the laboratory and bioinformatics protocol. In brief, we amplified markers of *c.* 500 bp in length (excluding primers), positioned in 3′ untranslated regions of protein-coding genes, in ten multiplex PCRs. Again, multiplexes for each individual were pooled and given unique tags. We sequenced the amplicons on the Illumina MiSeq next-generation sequencing platform to the average per base coverage of 1017 ± (SD) 1181. Sequence data were further processed using standard, freely available bioinformatic tools, producing phase-resolved variants. Fasta files were obtained from vcf files using custom python script. Marker-individual combinations with < 10 reads were considered failed. These data were previously used in another study (Zieliński *et al.*, 2016a).

Bayesian clustering analysis – constructing hypotheses

Triturus and *Lissotriton* newts hybridize with congeneric species at their contact zones (Arntzen, Wielstra & Wallis, 2014; Zieliński *et al.*, 2016a) and while introgression of mitochondrial DNA in *T. cristatus* is restricted to the contact zone with congeneric species (Wielstra *et al.*, 2015), it has led to the complete replacement of the original mitochondrial DNA of *L. montandoni* (Babik *et al.*, 2005; Zieliński *et al.*, 2013). Including individuals showing recent genetic admixture with another species (early generation hybrids) could have unpredictable effects in downstream analyses of intraspecific genetic divergence, while limited nuclear DNA introgression (via ancient hybridization) simply constitutes a part of intraspecific genetic diversity and as such does not require separate treatment in our models.

To confirm there were no early generation hybrids present in our data set, we took a two-step approach. We first used STRUCTURE 2.3.4 (Pritchard, Stephens & Donnelly, 2000) to confirm that our set of *T. cristatus* and *L. montandoni* individuals did not show significant genetic admixture (STRUCTURE $Q \geq 0.05$) with *Triturus* or *Lissotriton* species with abutting ranges. We did so by enforcing the number of gene pools (k) to 2 in pairwise species comparisons (Tables S1 and S2 in Supporting Information). Entire haplotypes were treated as alleles at each locus. We used the admixture model in combination with the correlated allele frequency model with 100 000 iterations, after 50 000 iterations of burn-in, and ran five replicates, which were summarized with CLUMPAK (Kopelman *et al.*, 2015). As *T. cristatus* has parapatric range boundaries with four other *Triturus* species, namely *T. carnifex*, *T. dobrogicus*, *T. ivanbureschi* and *T. macedonicus*, we took reference data for these species, four localities per species with three individuals per locality, from Wielstra *et al.* (2014). The only species that *L. montandoni* has a parapatric range boundary with is *L. vulgaris* and we took reference data for this species, 45 individuals from 38 localities, from Zieliński *et al.* (2016a).

Next, we used STRUCTURE to determine the number of intraspecific evolutionary lineages in both newt species. We used the same settings as before but tested over multiple values of k. The upper k limit was 35 for *T. cristatus* and 31 for *L. montandoni*, as defined by the total number of localities included. We used Evanno's Δk criterion (Evanno, Regnaut & Goudet, 2005) to select the optimum k value. The number of intraspecific lineages identified, and the allocation of localities to these lineages, were used to construct testable hypotheses on the spatial arrangement of glacial refugia in both newt species.

ABC – rationale

Using ABC, we evaluated the existence of three *T. cristatus* and two *L. montandoni* glacial refugia in the Carpathians (as suggested by STRUCTURE) by testing models assuming: (1) a Holocene (< 12 Ka) and (2) a Pleistocene (> 12 Ka) origin of intraspecific evolutionary lineages. Support for the latter model would imply that the evolutionary lineages diverged prior to the end of the last glacial maximum and hence must have survived glaciations in separate refugia. Therefore, our ABC modelling can be considered an explicit test of the refugia-within-refugia hypothesis. Within species, all parameter priors (except topology for *T. cristatus*) were identical for the tested models and no demographic changes and historical gene flow were allowed to keep models as simple as possible.

ABC – data preparation

For *T. cristatus*, we focus on localities in the Carpathian area only (1–28). According to the STRUCTURE results, crested newt localities were assigned to three lineages, one within (**TcB**), one east of (**TcE**) and one

south of (**TcS**) the Carpathian mountain belt (Fig. 1b). We considered three topologies: (1) (**TcE**, **TcS**) **TcB** – supported by a drift tree based on allele frequency data; (2) **TcB**, **TcE**, **TcS** – a polytomy; and (3) (**TcB**, **TcS**) **TcE** – supported by the nucleotide distance between evolutionary lineages (see Fig. S1 in Supporting Information). Two localities (2 and 9) showing a high degree of admixture between evolutionary lineages ($0.3 < Q < 0.7$) were not analysed to exclude the effect of ongoing hybridization and early generation admixture. Seven markers (*agl*, *clasp*, *gys*, *samdb*, *smo*, *taf8* and *usp*) in which more than 5% of individuals did not amplify were removed. Furthermore, 11 individuals for which one or more of the retained markers did not amplify were excluded. Next, alignment columns with missing data (i.e. indels) were removed. We assume that newt breeding ponds correspond to discrete demes which may undergo extinction and recolonization. To minimize the confounding effects of current population structure, we randomly subsampled one gene copy per locality. It has been shown (Wakeley & Aliacar, 2001; Wakeley, 2004) that if one gene copy per locus is sampled per deme in a metapopulation composed of a large number of demes, the ancestral process producing such a sample is identical to the unstructured coalescent process. Our final ABC data set contained one gene copy per locus from 25 localities, distributed over the three evolutionary lineages as follows: 7 **TcB**, 9 **TcE** and 9 **TcS**.

For *L. montandoni* STRUCTURE suggested two lineages: one south (**LmS**) and one north (**LmN**) of approximately the centre of the Eastern Carpathians, roughly the Ukrainian/Romanian border (Fig. 1c). As there are only two evolutionary lineages in *L. montandoni*, we only had to consider a single topology: **LmN**, **LmS** (Fig. S2 in Supporting Information). We excluded two individuals from localities with considerable admixture between evolutionary lineages ($0.3 < Q < 0.7$). For the ABC analysis, we excluded eight markers that were fully coding or amplified inconsistently so that the final data set included 66 markers. Furthermore, five individuals for which one or more of the retained markers did not amplify were excluded. Next, alignment columns with missing data were removed. As explained above for *T. cristatus*, one gene copy per marker was sampled per locality. Our final ABC data set contained one gene copy per locus from 24 localities, distributed over the two evolutionary lineages as follows: 9 **LmN** and 15 **LmS**.

ABC – SUMMARY STATISTICS

We focused on a set of basic summary statistics, likely to be informative about the time of the split between intraspecific evolutionary lineages, and other demographic parameters. For each evolutionary lineage, we calculated average and variance of: number of fixed polymorphisms (SF), number of shared polymorphisms (SS), number of private polymorphisms (SP), nucleotide F_{ST} (FST_nuc) calculated between evolutionary lineages and between a particular evolutionary lineage and the remaining ones pooled (in three-lineage models), Tajima's D (D), nucleotide diversity (Pi), number of haplotypes (nHap), haplotype diversity (HapW), d_{xy} calculated between lineages (PiA) and the number of haplotypes shared between all lineages and lineage pairs (n_shared_hap). Additionally, we calculated average and variance of nHap, HapW, D, Pi and the overall number of segregating sites (S) for the whole data set. Summary statistics for both observed and simulated data sets were calculated on polymorphic biallelic sites only. Positions with more than two segregating variants were excluded as departing from the infinite sites model. For each statistic, mean and variance across all loci were calculated using MSSTATSPOP v.0.998980-beta (Ramos-Onsins *et al.*, unpublished) and custom Python scripts.

ABC – SIMULATIONS AND ANALYSIS

Coalescent simulations were performed using FASTSIMCOAL2.01 (Excoffier *et al.*, 2013). We simulated data using the finite site mutation model (as our data did not fit the infinite site model) and a single, fixed mutation rate of $= 5.7 \times 10^{-9}$ per site, per generation, as previously estimated for smooth and Carpathian newts using fossil-based dating of divergence within genus *Lissotriton* (Pabijan *et al.*, 2015; Zieliński *et al.*, 2016a). Considering that *Triturus* and *Lissotriton* are relatively closely related (Zhang *et al.*, 2008) and we use highly similar genetic markers (Wielstra *et al.*, 2014; Zieliński *et al.*, 2014b), we considered it appropriate to use the same mutation rate for both systems. These markers are known to be unlinked in both newt systems (Zieliński *et al.*, 2016a; Wielstra *et al.*, 2017). Loci were simulated as independent chromosomes. The ABC analysis was performed within the ABCTOOLBOX (Wegmann *et al.*, 2010). We used a generation time of 4 years based on the synthesis of the literature (Nadachowska & Babik, 2009) and assumed it appropriate to use this value for *Triturus* as well (Duellman & Trueb, 1994). Our recombination rate priors were based on a previous estimate for smooth and Carpathian newts (Zieliński *et al.*, 2016a) (Tables S3 and S4 in Supporting Information). Parameter values were sampled from uniform prior distributions, priors for population sizes were uniform on a log10 scale (Tables S3 and S4 in Supporting Information) and were set to cover biologically plausible values. Analyses were based on 10^6 data sets simulated under

each demographic model. We retained the 0.1% (10^3) best simulations for each model and computed the marginal likelihood of the observed and retained data sets under a Generalized Linear Model (Leuenberger & Wegmann, 2010). For each species, we compared all models in a single model selection procedure and selected the best fitting ones based on posterior probabilities. We inspected posterior probability curves and the fraction of retained simulations with the marginal likelihood smaller or equal to that of the observed data (observed *P*-value) to determine if models could faithfully reproduce the observed data. The best fitting model was selected based on Bayes factors (ratios of model marginal densities). To estimate the power to distinguish between models, we generated 1000 pseudo-observed data sets for each model and checked how often the ABC model choice procedure correctly predicted the true model (the one that produced the data set). Each pseudo-observed data set was treated as the observed data and used to calculate marginal densities of all compared models. Bayes factors were then used to select the best model. As we were interested in both the overall power to identify the true model as well as the power in the observed summary statistics space, the pseudo-observed data sets for each model were chosen from both random and retained simulations. To check whether the marginal posterior distributions estimated from the best models were biased, we generated 1000 pseudo-observed data sets for each best model and tested uniformity of the posterior quantile distributions (the position of the true values within the posterior distribution) for each parameter with a Kolmogorov–Smirnoff test. If the parameter values for these pseudo-observed data were randomly chosen from the prior distribution, we expect the posterior quantiles to be uniformly distributed. Because for *T. cristatus* (while a Holocene divergence was confidently rejected) the posterior validation suggested potential overestimation of divergence time in the preferred model, we further explored this matter by rerunning the preferred model (1) without a fixed lower prior boundary for split time and (2) without a fixed lower prior boundary for split time and with an upper prior boundary for split time fixed to 0.5 Ma.

RESULTS

Bayesian clustering analysis – intraspecific evolutionary lineages

STRUCTURE confirmed our set of *T. cristatus* and *L. montandoni* individuals showed no significant recent genetic admixture with congenerics. STRUCTURE suggested $k = 3$ as the most likely number of gene pools for *T. cristatus* and $k = 2$ for *L. montandoni* (Tables S1 and S2 in Supporting Information). The three *T. cristatus* lineages roughly correspond to within (**TcB**), east of (**TcE**) and south of (**TcS**) the Carpathian mountain belt (Fig. 1b). Lineage **TcB** is also the one that postglacially colonized temperate Eurasia. The two *L. montandoni* lineages show a different geographical configuration, with an evolutionary lineage south (**LmS**) and north (**LmN**) of approximately the centre of the Eastern Carpathians, roughly the Ukrainian/Romanian border (Fig. 1c).

ABC – polymorphism and observed summary statistics

The *T. cristatus* ABC data set included 45 markers of the average length 139 bp (6248 bp). There were 106 haplotypes out of which 51 (48%) were shared between evolutionary lineages. We observed 67 polymorphic sites out of which four (6%) were private to **TcB**, 19 (28%) to **TcE** and 23 (34%) to **TcS**. The *L. montandoni* ABC data set comprised of 66 markers of the average length of 484 bp (31 929 bp). There were 391 haplotypes out of which 105 (27%) were shared between evolutionary lineages. We observed 652 polymorphic sites out of which 156 (24%) were private to **LmN** and 283 (43%) to **LmS**. In both species, the percent of sites segregating in all lineages was similar, 31% in *T. cristatus* and 33% in *L. montandoni*. We found no fixed differences between lineages in either species (Tables S5 and S6 in Supporting Information).

ABC – model choice for *Triturus cristatus*

The *P*-values calculated under the Generalized Linear Model were used to check whether tested models were able to reproduce the observed data (Table S5 in Supporting Information). For all *T. cristatus* models assuming a Pleistocene split (M2, M4, M6), the observed data fell well within the distribution of retained simulated data (Table S7 in Supporting Information). Models assuming a Pleistocene divergence were always favoured and the polytomy model (M4) had the highest posterior probability (PP = 0.95) (Table S7 in Supporting Information). The mean power to identify the true model was 0.59 and in the case of the preferred M4 model it was 0.74 (Table S9 in Supporting Information). Although within the observed summary statistics space the M4 model power decreased to 0.37, there was no case in which simulations produced under other models would choose M4 as the true model more often than the model of origin. Importantly, only simulations under other models of a Pleistocene divergence selected M4 more often than expected by chance (Table S9 in Supporting Information). The selected M4 model indicates a Middle Pleistocene 172 Ka (77–281

Ka) divergence between lineages (Fig. S3 and Table S3 in Supporting Information).

According to the posterior validation (Fig. S5 and Table S3 in Supporting Information), divergence time might be overestimated for model M4, so the estimates should be treated with caution. It needs to be stressed here, however, that hypothesis testing was based on model selection, not on parameter estimates. Therefore, the bias in the divergence time estimates does not affect the main results of our test, which firmly supports the Pleistocene divergence and rejects a Holocene divergence. Still, to interpret whether this bias affected the actual divergence time estimate within the preferred Pleistocene divergence model, we reran the preferred model without a fixed lower prior boundary for split time (M7) and without a fixed lower prior boundary for split time and with an upper prior boundary for split time fixed to 0.5 Ma (M8). While M7 showed a similar bias as M4, bias was considerably reduced in M8 (details on Dryad). Yet, the inferred divergence time was almost identical (details on Dryad). Hence, we conclude that the divergence time estimated in M4 is reliable.

ABC – MODEL CHOICE FOR *LISSOTRITON MONTANDONI*

A model assuming Pleistocene divergence (M2) performed better than one assuming post-Pleistocene divergence (M1; Table S8 in Supporting Information). The power to correctly predict the true model was high for both models, regardless of statistics space (Table S10 in Supporting Information). According to the Kolmogorov–Smirnoff test results (Table S4 in Supporting Information), all parameter distributions were biased. However, visual inspection of the distributions of divergence time posterior quantiles (Fig. S6 in Supporting Information) suggests that the true values were more often found in the centre of the distribution, which is a consequence of overly wide priors. Importantly, this kind of bias may only slightly decrease precision of the estimates. Hence, while our simple models were not able to faithfully reproduce the observed data (Tables S6 and S8 in Supporting Information), we nevertheless consider it safe to interpret the estimated divergence time from the best performing model. The selected M2 model again indicates a Middle Pleistocene 202 Ka (54–347 Ka) divergence between lineages (Fig. S4 and Table S4 in Supporting Information).

DISCUSSION

While the importance of the Carpathians as a glacial refugium has by now become well established, a more intricate pattern of refugia-within-refugia is still emerging (Mráz & Ronikier, 2016). We here tested the Carpathian refugia-within-refugia hypothesis, based on next-generation phylogeography and ABC analysis for two newt species of different genera. For both species, models assuming a Pleistocene divergence were strongly preferred, even though disparate patterns of intraspecific genetic structure highlight that species had idiosyncratic responses to glacial cycles (Fig. 1). The build-up of deep intraspecific differentiation in ecologically distinct species provides strong support for a scenario in which multiple discrete regions within the Carpathians acted as glacial refugia, for a broad range of species. Our findings emphasize the key role that the Carpathians played in Pleistocene survival and radiation of temperate Eurasia's biodiversity.

Accuracy of our divergence time estimates, crucial for the interpretation of this test, could be affected by (1) the mutation rate and generation time used to convert ABC estimates into calendar years, and (2) gene flow between evolutionary lineages. Only a several-fold underestimation of mutation time or overestimation of generation time could lead to erroneous support for Pleistocene divergence, but, as the values used are well supported, we consider this unlikely. Furthermore, gene flow would cause under- rather than an overestimation of divergence time, yet post-Pleistocene divergence was still rejected. Hence, we conclude that our ABC analysis strongly supports a pre-Pleistocene divergence of evolutionary lineages and provides robust evidence for Carpathian refugia-within-refugia, illustrating the added value of ABC analysis in Carpathian phylogeography (see also Kolář *et al.*, 2016).

Our nuclear DNA results suggest that the intraspecific structuring observed today originated during the penultimate glacial period (130–200 Ka). This is an order of magnitude younger than the divergence of the three mitochondrial DNA lineages present in *T. cristatus* (with even the most conservative interpretation based on confidence intervals suggesting divergence well over a million years ago), which have a similar distribution as the evolutionary lineages identified in the present study (Wielstra *et al.*, 2015). It should be noted that no comparable mitochondrial DNA data are available for *L. montandoni*, as its native mitochondrial DNA relatively recently got replaced with that of a congener, via mitochondrial DNA capture (Zieliński *et al.*, 2013). Nuclear gene flow upon secondary contact during Pleistocene interglacials would cause fusion of intraspecific lineages, a realistic scenario given the historical instability of phylogeographic patterns (Hofreiter *et al.*, 2004), and in fact genetic admixture is observed where evolutionary lineages meet today. Phylogeographic structure is often retained longer in mitochondrial DNA than in the nuclear genome (Petit & Excoffier, 2009). While the long-term

persistence of geographically structured mitochondrial DNA clades could be interpreted as evidence that the same areas acted as refugia during multiple glacial periods (Hewitt, 2011), our findings underline that the stability and historical isolation of refugia-within-refugia delineated based on mitochondrial DNA alone could well be overestimated. Considering the strong bias in phylogeographic surveys towards mitochondrial DNA (Riddle, 2016), we suggest that proposed refugia-within-refugia scenarios require re-evaluation with nuclear data.

ACKNOWLEDGEMENTS

B.W. initiated this work as a Newton International Fellow. This project has received funding from the European Union's Horizon 2020 research and innovation programme under the Marie Skłodowska-Curie grant agreement No. 655487. P.Z. and W.B. were supported by the Polish National Science Centre grants 8171/B/P01/2011/40 and 2014/15/B/NZ8/00250 and the Jagiellonian University grant DS/WBiNoZ/INoS/762/16. Samples were collected under permits: DOPozgiz-4200/II-78/3702/10/JRO provided by the Polish General Director for Environmental Protection, 03.04.12 No. 67 issued by the National Academy of Sciences of Ukraine and 3256/9.07.2010 provided by the Romanian Commission for Protection of Natural Monuments. Samples were collected with institutional animal ethics approval (number 101/2009), issued by the First Local Ethical Committee on Animal Testing at the Jagiellonian University in Krakow. J.W. Arntzen, M. Bonk, D. Cogălniceanu, S.-D. Covaciu-Marcov, K. Dudek, M. Herdegen, M. Liana, K. Nadachowska-Brzyska, Z. Prokop, J. Radwan and M. Stuglik helped with sampling. P. Kania and A. Fijarczyk provided python scripts. We thank two anonymous reviewers for their helpful comments.

REFERENCES

Abellán P, Svenning J-C. 2014. Refugia within refugia – patterns in endemism and genetic divergence are linked to Late Quaternary climate stability in the Iberian Peninsula. *Biological Journal of the Linnean Society* **113:** 13–28.

Arntzen JW, Wielstra B, Wallis GP. 2014. The modality of nine *Triturus* newt hybrid zones, assessed with nuclear, mitochondrial and morphological data. *Biological Journal of the Linnean Society* **113:** 604–622.

Babik W, Branicki W, Crnobrnja-Isailović J, Cogălniceanu D, Sas I, Olgun K, Poyarkov NA, Garcia-París M, Arntzen JW. 2005. Phylogeography of two European newt species – discordance between mtDNA and morphology. *Molecular Ecology* **14:** 2475–2491.

Canestrelli D, Bisconti R, Sacco F, Nascetti G. 2014. What triggers the rising of an intraspecific biodiversity hotspot? Hints from the agile frog. *Scientific Reports* **4:** 5042..

Duellman WE, Trueb L. 1994. *Biology of amphibians*. Baltimore, MD: JHU Press.

Evanno G, Regnaut S, Goudet J. 2005. Detecting the number of clusters of individuals using the software STRUCTURE: a simulation study. *Molecular Ecology* **14:** 2611–2620.

Excoffier L, Dupanloup I, Huerta-Sánchez E, Sousa VC, Foll M. 2013. Robust demographic inference from genomic and SNP data. *PLoS Genetics* **9:** e1003905.

Gómez A, Lunt DH. 2007. Refugia within refugia: patterns of phylogeographic concordance in the Iberian Peninsula. In: Weiss S and Ferrand N, eds. *Phylogeography of Southern European refugia*. Dordrecht: Springer, 155–188.

Hewitt G. 2000. The genetic legacy of the Quaternary ice ages. *Nature* **405:** 907–913.

Hewitt GM. 2011. Mediterranean peninsulas: the evolution of hotspots. In: Zachos FE and Habel JC, eds. *Biodiversity hotspots: distribution and protection of conservation priority areas*. Berlin: Springer, 123–147.

Hofreiter M, Serre D, Rohland N, Rabeder G, Nagel D, Conard N, Münzel S, Pääbo S. 2004. Lack of phylogeography in European mammals before the last glaciation. *Proceedings of the National Academy of Sciences of the United States of America* **101:** 12963–12968.

Kolář F, Fuxová G, Záveská E, Nagano AJ, Hyklová L, Lučanová M, Kudoh H, Marhold K. 2016. Northern glacial refugia and altitudinal niche divergence shape genome-wide differentiation in the emerging plant model *Arabidopsis arenosa*. *Molecular Ecology* **25:** 3929–3949.

Kopelman NM, Mayzel J, Jakobsson M, Rosenberg NA, Mayrose I. 2015. Clumpak: a program for identifying clustering modes and packaging population structure inferences across K. *Molecular Ecology Resources* **15:** 1179–1191.

Leuenberger C, Wegmann D. 2010. Bayesian computation and model selection without likelihoods. *Genetics* **184:** 243–252.

Mráz P, Ronikier M. 2016. Biogeography of the Carpathians: evolutionary and spatial facets of biodiversity. *Biological Journal of the Linnean Society* **119:** 528–559.

Nadachowska K, Babik W. 2009. Divergence in the face of gene flow: the case of two newts (Amphibia: Salamandridae). *Molecular Biology and Evolution* **26:** 829–841.

Pabijan M, Zieliński P, Dudek K, Chloupek M, Sotiropoulos K, Liana M, Babik W. 2015. The dissection of a Pleistocene refugium: phylogeography of the smooth newt, *Lissotriton vulgaris*, in the Balkans. *Journal of Biogeography* **42:** 671–683.

Petit RJ, Excoffier L. 2009. Gene flow and species delimitation. *Trends in Ecology & Evolution* **24:** 386–393.

Poulakakis N, Kapli P, Lymberakis P, Trichas A, Vardinoyiannis K, Sfenthourakis S, Mylonas M. 2015. A review of phylogeographic analyses of animal taxa from the Aegean and surrounding regions. *Journal of Zoological Systematics and Evolutionary Research* **53:** 18–32.

Pritchard JK, Stephens M, Donnelly P. 2000. Inference of population structure using multilocus genotype data. *Genetics* **155:** 945–959.

Ramos-Onsins SE, Ferretti L, Raineri E, Jené J, Marmorini G, Burgo W, Vera G. Unpublished. *Mstatspop: statistical analysis using multiple populations for genomic data*. Available at: https://bioinformatics.cragenomica.es/numgenomics/people/sebas/software/software.html

Riddle BR. 2016. Comparative phylogeography clarifies the complexity and problems of continental distribution that drove A. R. Wallace to favor islands. *Proceedings of the National Academy of Sciences* **113:** 7970–7977.

Schmitt T, Varga Z. 2012. Extra-Mediterranean refugia: the rule and not the exception? *Frontiers in Zoology* **9:** 22.

Speybroeck J, Beukema W, Bok B, Van Der Voort J. 2016. *Field guide to the amphibians and reptiles of Britain and Europe*. London: Bloomsbury Publishing.

Stewart JR, Lister AM, Barnes I, Dalen L. 2010. Refugia revisited: individualistic responses of species in space and time. *Proceedings of the Royal Society B-Biological Sciences* **277:** 661–671.

Wakeley J. 2004. Metapopulation models for historical inference. *Molecular Ecology* **13:** 865–875.

Wakeley J, Aliacar N. 2001. Gene genealogies in a metapopulation. *Genetics* **159:** 893–905.

Wegmann D, Leuenberger C, Neuenschwander S, Excoffier L. 2010. ABCtoolbox: a versatile toolkit for approximate Bayesian computations. *BMC Bioinformatics* **11:** 116.

Wielstra B, Babik W, Arntzen JW. 2015. The crested newt *Triturus cristatus* recolonized temperate Eurasia from an extra-Mediterranean glacial refugium. *Biological Journal of the Linnean Society* **114:** 574–587.

Wielstra B, Burke T, Butlin RK, Avcı A, Üzüm N, Bozkurt E, Olgun K, Arntzen JW. 2017. A genomic footprint of hybrid zone movement in crested newts. *Evolution Letters* **1:** 93–101.

Wielstra B, Crnobrnja-Isailović J, Litvinchuk SN, Reijnen BT, Skidmore AK, Sotiropoulos K, Toxopeus AG, Tzankov N, Vukov T, Arntzen JW. 2013. Tracing glacial refugia of *Triturus* newts based on mitochondrial DNA phylogeography and species distribution modeling. *Frontiers in Zoology* **10:** 13.

Wielstra B, Duijm E, Lagler P, Lammers Y, Meilink WR, Ziermann JM, Arntzen JW. 2014. Parallel tagged amplicon sequencing of transcriptome-based genetic markers for *Triturus* newts with the Ion Torrent next-generation sequencing platform. *Molecular Ecology Resources* **14:** 1080–1089.

Wielstra B, Zieliński P, Babik W. 2017. Data from: The Carpathians hosted extra-Mediterranean refugia-within-refugia during the Pleistocene Ice Age: genomic evidence from two newt genera. *Dryad Digital Repository*. http://dx.doi.org/10.5061/dryad.1m1hg

Zhang P, Papenfuss TJ, Wake MH, Qu L, Wake DB. 2008. Phylogeny and biogeography of the family Salamandridae (Amphibia: Caudata) inferred from complete mitochondrial genomes. *Molecular Phylogenetics and Evolution* **49:** 586–597.

Zieliński P, Dudek K, Stuglik MT, Liana M, Babik W. 2014a. Single nucleotide polymorphisms reveal genetic structuring of the Carpathian newt and provide evidence of interspecific gene flow in the nuclear genome. *PLoS One* **9:** e97431.

Zieliński P, Nadachowska-Brzyska K, Dudek K, Babik W. 2016a. Divergence history of the Carpathian and smooth newts modelled in space and time. *Molecular Ecology* **25:** 3912–3928.

Zieliński P, Nadachowska-Brzyska K, Dudek K, Babik W. 2016b. Data from: Divergence history of the Carpathian and smooth newts modelled in space and time. *Dryad Digital Repository*. http://dx.doi.org/10.5061/dryad.83k00.

Zieliński P, Nadachowska-Brzyska K, Wielstra B, Szkotak R, Covaciu-Marcov SD, Cogălniceanu D, Babik W. 2013. No evidence for nuclear introgression despite complete mtDNA replacement in the Carpathian newt (*Lissotriton montandoni*). *Molecular Ecology* **22:** 1884–1903.

Zieliński P, Stuglik MT, Dudek K, Konczal M, Babik W. 2014b. Development, validation and high-throughput analysis of sequence markers in nonmodel species. *Molecular Ecology Resources* **14:** 352–360.

SUPPORTING INFORMATION

Additional Supporting Information may be found in the online version of this article at the publisher's web-site:

Figure S1. The six models tested in an approximate Bayesian computation framework for *Triturus cristatus*. M1 and M2 apply a (TcE, TcS) TcB topology, M3 and M4 a polytomy, and M5 and M6 a (TcB, TcS) TcE topology. M1, M3 and M5 assume a Holocene (< 12 Ka) and M2, M4 and M6 a Pleistocene (> 12 Ka) origin of intraspecific evolutionary lineages. NTcB, NTcE, NTcS, NTcES, NTcBS, Nanc represent population size of TcB, TcE, TcS, the ancestral population of TcE and TcS, the ancestral population of TcB and TcS, and the ancestral population of all lineages. TS(ES), TS(BS) and TS represent time of split of ancestral population of TcE and TcS, the ancestral population of TcB and TcS, and the ancestral population of all lineages. The selected model is framed.

Figure S2. The two models tested in an approximate Bayesian computation framework for *Lissotriton montandoni*. M1 assumes a Holocene (< 12 Ka) and M2 a Pleistocene (> 12 Ka) origin of intraspecific evolutionary lineages. NLmN, NLmS and Nanc represent the population size of LmN, LmS and the ancestral population of both lineages. TS represents the time of split of the ancestral population of all lineages. The selected model is framed.

Figure S3. Posterior probabilities of the parameters inferred from the best model (M4) for *Triturus cristatus*. Black = prior distribution; blue = parameter distribution among the retained simulations; red = obtained posterior

distribution. NTcB, NTcE, NTcS, Nanc are the population size of TcB, TcE, TcS and the ancestral population of all lineages. Population sizes are given on log10 scale. TS represents the time of split of ancestral population of all lineages. r is the recombination rate between adjacent sites.

Figure S4. Posterior probabilities of the parameters inferred from the best model (M2) for *Lissotriton montandoni*. Black = prior distribution; blue = parameter distribution among the retained simulations; red = obtained posterior distribution. NLmN, NLmS and Nanc represent the population sizes of LmN, LmS and the ancestral population of both lineages. Population sizes are given on log10 scale. TS represents the time of split of ancestral population of both lineages. r is the recombination rate between adjacent sites.

Figure S5. Distributions of posterior quantiles of all the parameters inferred from the best model (M4) for *Triturus cristatus*. Posterior quantiles should be uniformly distributed if the posteriors are unbiased. NTcB, NTcE, NTcS, Nanc represent the population size of TcB, TcE, TcS and the ancestral population of all lineages. Population sizes are given on log10 scale. TS represents the time of split of ancestral population of all lineages. r is the recombination rate between adjacent sites.

Figure S6. Distributions of posterior quantiles of all the parameters inferred from the best model (M2) for *Lissotriton montandoni*. Posterior quantiles should be uniformly distributed if the posteriors are unbiased. NLmN, NLmS, Nanc represent the population size of LmN, LmS and the ancestral population of both lineages. Population sizes are given on log10 scale. TS represents the time of split of ancestral population of both lineages. r is the recombination rate between adjacent sites.

Table S1. Results of the STRUCTURE analysis for *Triturus cristatus*.

Table S2. Results of the STRUCTURE analysis for *Lissotriton montandoni*.

Table S3. *Triturus cristatus* M4 priors and posteriors.

Table S4. *Lissotriton montandoni* M2 priors and posteriors.

Table S5. *Triturus cristatus* observed summary statistics.

Table S6. *Lissotriton montandoni* observed summary statistics.

Table S7. *Triturus cristatus* model performance.

Table S8. *Lissotriton montandoni* model performance.

Table S9. *Triturus cristatus* model power.

Table S10. *Lissotriton montandoni* model power.

SHARED DATA

Sequence data and files associated with analyses are available from the Dryad Digital Repository: Zieliński *et al.* (2016b) and Wielstra, Zieliński & Babik (2017).